

# Study of QCD dynamics using small systems

Suman Deb,<sup>\*</sup> Golam Sarwar,<sup>†</sup> and Raghunath Sahoo<sup>‡</sup>

*Department of Physics, Indian Institute of Technology Indore, Simrol, Indore 453552, INDIA*

Jan-e Alam<sup>§</sup>

*Variable Energy Cyclotron Centre, 1/AF, Bidhan Nagar, Kolkata - 700064, India*

(Dated: June 18, 2021)

The multiplicity, finite system size and collision energy dependence of heat capacity ( $C_V$ ), conformal symmetry breaking measure (CSBM) and speed of sound ( $c_s$ ) have been investigated using ALICE data for  $p + p$  collisions at  $\sqrt{s} = 7$  TeV. The aim of this study is to ascertain the possibility of formation of a thermalized medium in such collisions. We find that there is a threshold in charged particle multiplicity beyond which  $C_V$ , CSBM and  $c_s$  attain plateau. The presence of such threshold in multiplicity is further reflected in the variation of these quantities with center-of-mass energy ( $\sqrt{s}$ ). In order to have a grasp on experimentally obtained results, variation of average transverse momentum with multiplicity has also been studied. The experimental results have been contrasted with PYTHIA8 and it is found that PYTHIA8 is inadequate to explain the features reflected in these quantities, thereby indicating the possibility of thermalization in such small system. It is also observed that the finite size effects alone cannot explain the non-extensive nature of particle spectra in  $p + p$  collisions.

PACS numbers:

## I. INTRODUCTION

One of the main goals of relativistic heavy-ion collision experiments (RHICE) is to create and characterize quark gluon plasma (QGP). QGP is a deconfined state of quarks and gluons which can be realized at high density and temperature. It is expected that such high density and temperature can be created by colliding nuclei at relativistic energies. The characterization of QGP (i.e, determination of its equation of state, transport properties, etc.) can be done by analyzing experimental data with the help of theoretical models. But the applicability of these theoretical models relies on certain assumptions. For example, relativistic dissipative hydrodynamics [1] can be used to analyze experimental data on anisotropic flow for the estimation of the viscous coefficients of QGP. Currently, it is not possible to prove from the first principle that the system produced in RHICE has achieved thermal equilibrium. Therefore, study on the validity of the assumption of local thermalization (and hence applicability of hydrodynamics) with the help of experimental data is crucial.

The assumption for the formation of partonic medium in RHICE is substantiated by experimental observations such as non-zero collective flow [2], suppression of  $J/\psi$  yield [3], enhancement of strangeness [4], suppression of high transverse momentum ( $p_T$ ) hadrons [5], etc. These

observations have been attributed to the formation of locally thermalized partonic medium which hydrodynamically evolves in space and time. Several parameters which are used to characterize the QGP formed in RHICE have been extracted by analyzing experimental data where data from  $p + p$  collision has been used as a benchmark. However, when small systems formed in high-multiplicity  $p + p$  collisions show long-range “ridge” in two particle azimuthal correlations with a large pseudorapidity separation [6–11] imitating collectivity, then the role of  $p + p$  collisions as a benchmark becomes obscured (although it is shown that non-medium effects can explain the features [12, 13]). In this regard, it is important to understand the role of the number of constituents for the formation of the QCD medium and  $p + p$  collisions can serve as a platform to address such issues. The multiplicity serves as a proxy to the number of constituents in a system formed in  $p + p$  collisions. It may be recalled that the issue of thermalization in small systems was studied in 1953 by Landau [14] and in 1982, van Hove investigated thermalization and quark-hadron phase transition in proton-antiproton collisions using variation of average  $p_T$  ( $\langle p_T \rangle$ ) with multiplicity [15]. Recently, QCD thermodynamics in  $p + p$  collisions has been studied in [16].

The purpose of this work is to investigate - how some of the markers of thermalization *e.g.* the thermodynamic quantities like,  $C_V$ , CSBM and  $c_s$  for small system vary with the quantities like multiplicity, size and collision energy. Because the chances for the system to achieve thermalization will increase with the increase of these quantities. Therefore, any change in the variation of  $C_V$ , CSBM and  $c_s$  with multiplicity (say) which is different from the change obtained from Monte-Carlo generators, which is devoid of thermalization (PYTHIA8 here) will signal on the possibility of thermalization. These quantities have

---

<sup>\*</sup>Electronic address: sumandeb0101@gmail.com

<sup>†</sup>Electronic address: golamsarwar1990@gmail.com

<sup>‡</sup>Electronic address: Raghunath.Sahoo@cern.ch (Corresponding author, Presently CERN Scientific Associate, CERN, Geneva, Switzerland)

<sup>§</sup>Electronic address: jane@vecc.gov.in

been chosen because  $C_V$  is one of the most basic and commonly used quantities which records the response of the system subjected to temperature stimulus. Similarly,  $c_s$  provides the information on the equation of state of a thermal medium and the CSBM, which can be expressed in terms of energy density ( $\epsilon$ ), pressure ( $P$ ) and temperature ( $T$ ) as CSBM =  $(\epsilon - 3P)/T^4$  (see [17, 18] for details). In this context the variation of  $\langle p_T \rangle$  of the hadrons with multiplicity connected to the temperature and entropy of a thermal system respectively will also be examined. As there is no way to directly probe, the spectra of produced hadrons are used to gain insight about the possible partonic phase. The ALICE data for  $p + p$  collisions at  $\sqrt{s} = 7$  TeV have been used to obtain  $C_V$ , CSBM and  $c_s$  and the results have been contrasted with PYTHIA8. The analysis using PYTHIA8 shows some degree of success in explaining some of the observations made in  $p + p$  and  $p + \text{Pb}$  collisions, such as saturation of  $\langle p_T \rangle$  of  $J/\psi$  [19, 20] and that of charged particles [21], as a function of charged particle multiplicity [22]. Though variation of heat capacity with collision energy has been investigated [23, 24] through temperature fluctuations for systems formed in RHICE, we are not aware of any studies in literature similar to the present one for small systems formed in  $p + p$  collisions for understanding thermalization.

The paper is organized as follows. Formalism used in this work has been presented in section II. Section III is devoted to discuss the methodology used for event generation in PYTHIA8. Results and discussions are presented in section IV. Finally in section V, we present the summary of our results.

## II. FORMALISM

We will recall some of the well-known thermodynamic relations in this section. The system formed at the LHC energies at the central rapidity region will be dominated by gluons, which neither carry electric nor baryonic charges. Such a system can be described by one single thermodynamic variable, the temperature ( $T$ ).

Now we would like to quote the standard thermodynamic expressions [25] for  $C_V$ ,  $c_s^2$  and entropy density ( $s$ ) below for a system with vanishing chemical potential as:

$$C_V = \left( \frac{\partial \epsilon}{\partial T} \right)_V, \quad (1)$$

$$s = \left( \frac{\partial P}{\partial T} \right)_V, \quad (2)$$

$$c_s^2 = \left( \frac{\partial P}{\partial \epsilon} \right)_s = s/C_V, \quad (3)$$

where  $V$  is the volume of the system. Now it is clear that to estimate the thermodynamic quantities of our interest we need to know  $\epsilon$ ,  $P$ ,  $s$ , etc and these quantities can be calculated by using the phase space distribution functions ( $f(E)$ ) [26]. Interestingly,  $f(E)$  for different hadrons can be measured experimentally by detecting their momentum distribution functions which allows us to connect data with  $C_V$ ,  $c_s$ , CSBM etc.

In the present work the Tsallis non-extensive statistics [27] is used to reproduce the  $p_T$ -spectra of hadrons at kinetic freeze-out [28–30]. The Tsallis-Boltzmann (TB) distribution function [31–33] has been widely used to describe the results from RHICE. The TB distribution is given by:

$$f(E) \equiv \frac{1}{\exp_q\left(\frac{E}{T}\right)} \quad (4)$$

where,

$$\exp_q(x) \equiv \begin{cases} [1 + (q-1)x]^{\frac{1}{q-1}} & \text{if } x > 0 \\ [1 + (1-q)x]^{\frac{1}{1-q}} & \text{if } x \leq 0 \end{cases} \quad (5)$$

where  $x = E/T$ ,  $E$  is the energy ( $E = \sqrt{p^2 + m^2}$ ),  $p$  and  $m$  are momentum and mass of the particle, respectively. It is important to note that in the limit,  $q \rightarrow 1$ , Eq. (5) reduces to the standard exponential function,

$$\lim_{q \rightarrow 1} \exp_q(x) \rightarrow \exp(x).$$

$T$  and  $q$  appearing in TB distribution are extracted by fitting experimental data on hadronic  $p_T$ -spectra with this distribution. The parameter  $q$  is called the non-extensive parameter which is a measure of degree of deviation from Boltzmann-Gibbs (BG) statistics. and  $T$  appearing in this formalism obeys the fundamental thermodynamic relation:

$$T = \frac{\partial U}{\partial S} \Big|_{N,V}, \quad (6)$$

where  $U$  is the internal thermal energy,  $S$  is the total entropy ( $= sV$ ),  $N$  is the number of particles and hence, the parameter  $T$  can be called temperature, even though the system obeys the Tsallis and not the BG statistics.

The calculation of the number density ( $n$ ), energy density ( $\epsilon$ ), pressure ( $P$ ) from the thermal phase space density,  $f(E)$  is straight forward [26]. These are given by,  $n = g/(2\pi)^3 \int d^3p f(E)$ ,  $\epsilon = g/(2\pi)^3 \int d^3p E f(E)$  and  $P = g/(2\pi)^3 \int d^3p \frac{p^2}{3E} f(E)$ . Analogously  $\epsilon$ ,  $P$ , etc can be estimated for TB distribution by inserting  $f(E)$  from Eq. 4. The expression for energy density ( $\epsilon$ ) then reads as [34, 35]:

$$\begin{aligned} \epsilon = & \frac{g}{2\pi^2} \int dp p^2 \sqrt{p^2 + m^2} \\ & \times \left[ 1 + \frac{(q-1)\sqrt{p^2 + m^2}}{T} \right]^{-\frac{q}{q-1}}, \end{aligned} \quad (7)$$

where,  $g$  is the degeneracy factor.

Similarly the expression for pressure ( $P$ ) is given by [34, 35]:

$$P = \frac{g}{2\pi^2} \int dp p^4 \frac{1}{3\sqrt{(p^2 + m^2)}} \times \left[ 1 + \frac{(q-1)\sqrt{(p^2 + m^2)}}{T} \right]^{\frac{-q}{q-1}}, \quad (8)$$

The expression for  $C_V$  as given in Eq. 1 can be obtained from Eq. 7 as:

$$C_V = \frac{qg}{2\pi^2 T^2} \int dp p^2 (p^2 + m^2) \times \left[ 1 + \frac{(q-1)\sqrt{(p^2 + m^2)}}{T} \right]^{\frac{1-2q}{q-1}}, \quad (9)$$

The dimensionless quantity  $I/T^4$ , where  $I = \epsilon - 3P$  called the trace anomaly [17, 18] or CSBM can be expressed as:

$$\frac{I}{T^4} = \frac{g}{2\pi^2 T^4} \int dp p^2 \sqrt{(p^2 + m^2)} \left[ 1 - \frac{p^2}{(p^2 + m^2)} \right] \times \left[ 1 + \frac{(q-1)\sqrt{(p^2 + m^2)}}{T} \right]^{\frac{-q}{q-1}}, \quad (10)$$

The squared velocity of sound ( $c_s^2$ ) in QGP is given by:

$$c_s^2 = \frac{qg}{6\pi^2 T^2} \frac{\int dp p^4 \times \left[ 1 + \frac{(q-1)\sqrt{(p^2 + m^2)}}{T} \right]^{\frac{1-2q}{q-1}}}{C_V} \quad (11)$$

and finally, the  $\langle p_T \rangle$  for the TB distribution can be estimated from the following expression:

$$\langle p_T \rangle = \frac{\int dp_T p_T^2 f(E)^q}{\int dp_T p_T f(E)^q}. \quad (12)$$

*i.e.*

$$\langle p_T \rangle = \frac{\int dp_T p_T^2 \left[ 1 + (q-1) \frac{\sqrt{(p_T^2 + m^2)}}{T} \right]^{\frac{-q}{q-1}}}{\int dp_T p_T \left[ 1 + (q-1) \frac{\sqrt{(p_T^2 + m^2)}}{T} \right]^{\frac{-q}{q-1}}}. \quad (13)$$

### III. EVENT GENERATION AND ANALYSIS METHODOLOGY

In order to make a comparative study, results obtained in this work are compared with QCD-inspired Monte-Carlo generator PYTHIA8, which is an amalgam of various physics mechanisms like hard and soft interactions, initial and final-state parton showers, fragmentation, multipartonic interactions, color reconnection, rope hadronization etc [36]. This model is used here to simulate  $p+p$  collisions at ultra-relativistic energies. Detailed explanation on PYTHIA8 physics processes and their implementation can be found in Ref.[37].

We have used 8.215 version of PYTHIA, which includes multi-partonic interaction (MPI). MPI is crucial to explain the underlying events multiplicity distributions. Also, this version includes color reconnection which mimics the flow-like effects in pp collisions [38]. It is crucial to mention here that PYTHIA8 does not have in-built thermalization. However, as reported in Ref. [38], the color reconnection (CR) mechanism along with the multipartonic interactions (MPI) in PYTHIA8 produces the properties which mimics thermalization of a system such as radial flow and mass dependent rise of mean transverse momentum. Apparently the PYTHIA8 with MPI and CR has the ability to produce the features similar to thermalization.

QCD processes in PYTHIA8 are categorised as soft and hard QCD processes, where production of heavy quarks are included in the latter. We have simulated the inelastic, non-diffractive component of the total cross-section for all the soft QCD process (SoftQCD:all = on) and Hard QCD process (HardQCD:all = 0) separately. MPI based scheme of color reconnection (ColorReconnection:reconnect =0) are also included. We have generated 100 million events with 4C tune (Tune:pp=5) [39], which give sufficient statistics to obtain  $p_T$ -spectra even in high-multiplicity events. To check the compatibility of tunes used in this work, we have compared simulated results obtained from hard and soft QCD tune of PYTHIA8 with the experimental data [40] as shown in Fig. 1. Here, we have compared PYTHIA8 simulated data with ATLAS data [40] as at the time of this work, there is no mini-biased ALICE data available for transverse momentum distribution of charged particles in  $p+p$  collisions at  $\sqrt{s}=7$  TeV. The motivation to contrast the PYTHIA8 generated results with the experimental data is to show that the soft processes fit the data reasonably well as shown in Fig 1. This comparison makes it clear that softQCD tune of the PYTHIA8 is suitable for the present work.

The generated events are categorised into seven multiplicity bins as (0-2), (2-4), (4-8), (8-11), (11-14), (14-18), (18-24) from which charged-particle pseudorapidity densities ( $\langle dN_{ch}/d\eta \rangle$ ) at mid-rapidity are obtained. The  $p_T$  distribution generated by PYTHIA8 for different multiplicity bins are now fitted with the following expression with  $T$  and  $q$  as fitting parameter [41]:

$$\frac{1}{p_T} \frac{d^2 N}{dp_T dy} \Big|_{y=0} = \frac{gV m_T}{(2\pi)^2} \left[ 1 + (q-1) \frac{m_T}{T} \right]^{-\frac{q}{q-1}}, \quad (14)$$

where  $m_T = \sqrt{p_T^2 + m^2}$ . The fitting parameters,  $T$  and  $q$  depends on the mass of the hadrons.

The  $p_T$ -spectra of  $\pi^\pm$ ,  $K^\pm$ ,  $K^{*0} + \bar{K}^{*0}$  and  $p + \bar{p}$  from simulated data at the mid-rapidity ( $|\eta| < 0.5$ ) for different multiplicity bins in  $p+p$  collisions at  $\sqrt{s} = 7$  TeV have been considered. The fitting of the PYTHIA8 generated spectra by Eq. 14 is displayed in Fig. 2. Figure 3 shows the quality of fitting in terms of  $\chi^2/NDF$  as function of multiplicity which shows that the quality of

fitting is reasonably good for all the particles under consideration at all multiplicity classes except for  $p + \bar{p}$  at low multiplicity class.

Figures 4 and 5 show the comparison of the parameters  $T$  and  $q$  extracted from the experimental data and the PYTHIA8 generated results for different charged particle multiplicities [42, 43].

With the detailed analysis methodology and  $(T, q)$  values obtained from PYTHIA8, we now move to discuss the results obtained by comparing ALICE experimental data and simulated data in the next section.

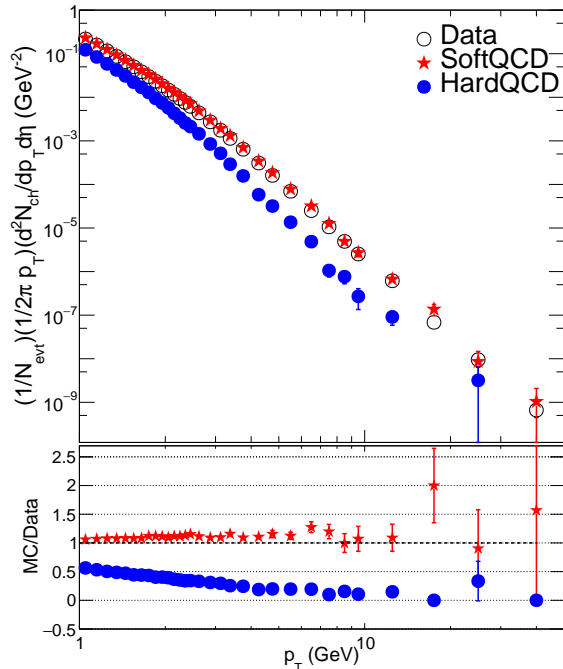


FIG. 1: (Color online) The upper panel shows the comparison of experimental data [40], HardQCD and SoftQCD tunes of PYTHIA8 for  $p+p$  collisions at  $\sqrt{s} = 7$  TeV. The black open circles are experimental data, red stars and blue solid circles are PYTHIA8 simulated data with SoftQCD and HardQCD tunes, respectively. The lower panel shows the ratio of PYTHIA8 to experimental data for both softQCD and hardQCD cases. The vertical lines indicate the error bars.

#### IV. RESULTS AND DISCUSSIONS

The thermodynamic quantities,  $C_V$ , CSBM,  $c_s$  and  $\langle p_T \rangle$  can be estimated by using Eqs. 9, 10, 11, and 13 with the values of  $T$  and  $q$  extracted by parameterizing the  $p_T$  spectra of identified hadrons using TB distribution. We note that a similar kind of approach has been used to study the variation of  $C_V$  with  $\sqrt{s_{NN}}$  at the freeze-out surfaces in the context of heavy-ion collisions [23]. The ALICE data on the  $p_T$ -spectra originating from  $p + p$  collisions at 7 TeV collision energy [44]

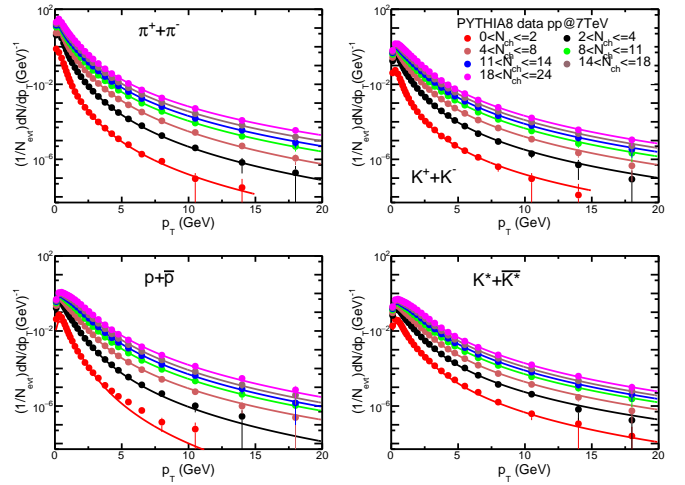


FIG. 2: (Color online) Fitting of PYTHIA8 generated  $p_T$ -spectra of  $\pi^\pm$ ,  $K^\pm$ ,  $K^{*0} + \bar{K}^{*0}$  and  $p + \bar{p}$  using Tsallis distribution (Eq. 14) for various multiplicity classes at mid-rapidity for  $p + p$  collisions at  $\sqrt{s} = 7$  TeV. In the legend of the figure, we have used a short notation  $N_{ch}$  for  $\langle dN_{ch}/d\eta \rangle$ .

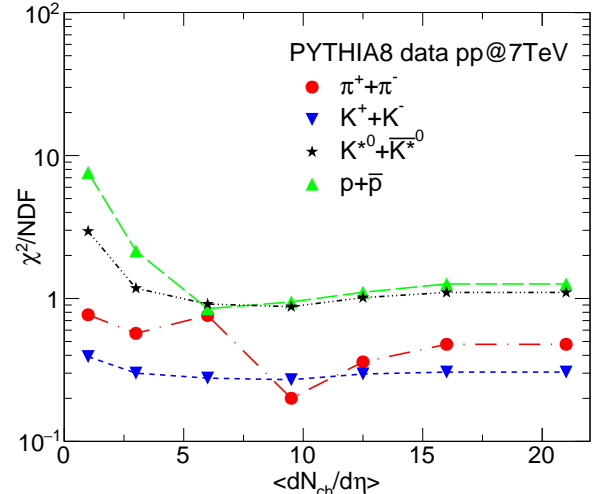


FIG. 3: (Color online)  $\chi^2/\text{NDF}$  for  $\pi^\pm$ ,  $K^\pm$ ,  $K^{*0} + \bar{K}^{*0}$  and  $p + \bar{p}$  as a function of charged particle multiplicity obtained by fitting Tsallis distribution (Eq. 4).

have been used to extract the values of  $T$  and  $q$  for each multiplicity in Ref. [43]. It is found that the values of  $T$  and  $q$  depend on hadronic species hinting at different decoupling or freeze out temperature for different hadrons [42]. In general, the hadrons with higher inverse slope (of  $p_T$ -spectra) is expected to come either from early stage and/or suffer more transverse flow. In the present study, we consider hadronic spectra of pion ( $\pi^\pm$ ), kaon ( $K^\pm$ ), neutral kstar ( $K^{*0} + \bar{K}^{*0}$ ) and proton ( $p + \bar{p}$ ).

The variation of  $C_V$ ,  $C_V/\langle n_i \rangle$ , (where  $i = \pi^\pm, K^\pm,$

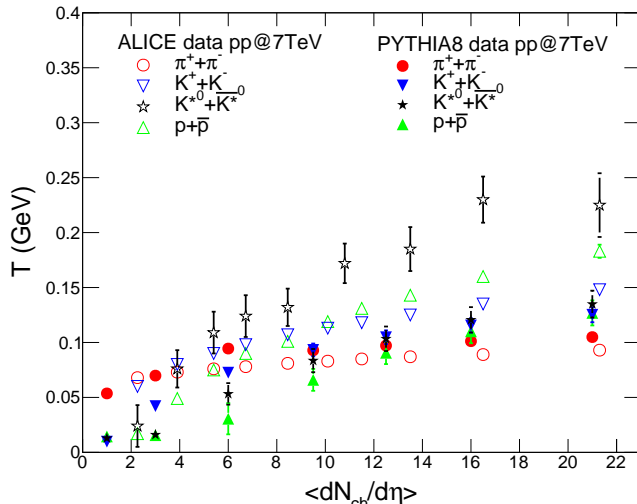


FIG. 4: (Color online) Multiplicity dependence of  $T$  for  $p + p$  collisions at  $\sqrt{s} = 7$  TeV obtained by using Eq. 14 as a fitting function for the PYTHIA8 simulated numbers (solid markers) and experimental data (open markers) [43].

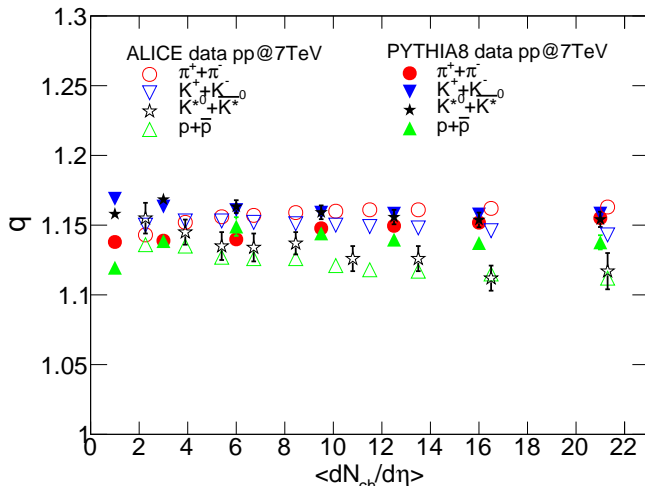


FIG. 5: (Color online) Same as Fig.4 for variation of the parameter  $q$  with charged particle multiplicity.

$K^{*0} + \bar{K}^{*0}$  and  $p + \bar{p}$ ),  $C_V/T^3$ ,  $C_V/(\epsilon + P)$ , CSBM,  $c_s^2$  and  $\langle p_T \rangle$  with  $\langle dN_{ch}/d\eta \rangle$  at mid-rapidity have been considered. Here  $\langle n_i \rangle$  (in  $\text{GeV}^3$ ) is the number density (number per unit volume) of the hadron  $i$ , obtained by integrating Eq. 4 over three momentum and  $(\epsilon + P)$  is the enthalpy density. The values of  $\langle dN_{ch}/d\eta \rangle$  obtained in the experiment for different multiplicity classes tabulated in table I (see Ref. [44] for details). We also investigate whether finite system size alone can account for non-extensivity observed in the spectra. To make a distinction between systems with and without thermal-

ization we contrast the results with the PYTHIA8 simulated outputs under the same collision condition.

### A. Multiplicity dependence of heat capacity

As mentioned before,  $C_V$  is one of the most fundamental quantities that gives the response of a thermal system under the influence of temperature stimulus. It gives the measure of how variation of temperature changes the entropy of a system ( $\Delta S = \int \frac{C_V}{T} dT$ ). The change in entropy is a good observable for studying the phase transition. In the context of heavy-ion collisions, entropy ( $S$ ) per unit rapidity ( $y$ ),  $dS/dy$  can be connected to the the corresponding multiplicity ( $dN/dy$ ). Therefore, the heat capacity acts as bridging observable for experimental measurement and theoretical models. For a strongly interacting system sufficient heat energy should be supplied to overcome the ‘binding force’ caused by the interaction to increase the temperature *i.e.* to supply adequate randomized kinetic energy by the constituents of the system. In other words, the mechanism of randomization to increase the temperature will require supply of more heat energy for strongly interacting system compared to that needed for the weakly interacting system. That is heat energy supplied to the strongly interacting system will not be entirely utilized to increase the temperature, some amount will be used to weaken the binding. Hence the increase in temperature in a strongly interacting system will be less than a weakly interacting system for a given amount of energy supplied to the system. Thus, the heat capacity bears the effects of strength of interaction among constituents of the system and represents the ease of randomization for the particular phase of the matter. Therefore, for weakly interacting gas increase of temperature has negligible effects on change in interaction strength. As a result its scaled value,  $C_V/\langle n_i \rangle$  will display a plateau. This makes heat capacity a good observable to study how correlation and randomization competes in the system. The variation of heat with multiplicity in  $p + p$  collision gives opportunities to better understand the randomization and the change in the strength of correlation with number of constituents in the QCD system.

The variation of  $C_V$  with  $\langle dN_{ch}/d\eta \rangle$  for  $\pi^\pm$ ,  $K^\pm$ ,  $K^{*0} + \bar{K}^{*0}$  and  $p + \bar{p}$  extracted from ALICE data has been displayed in Fig. 6. The result has been contrasted with the output obtained from PYTHIA8 simulation at the same  $p + p$  colliding energy. It is observed that results from PYTHIA8 which do not contain medium effects differ from data. Also, it is noted that the heat capacity increases with increase in multiplicity. If a thermalized medium is formed, then, in the ideal gas limit, heat capacity varies linearly with number of particles ( $C_V \propto \langle n_i \rangle$ ).

Therefore, in Fig. 7 we depict the variation of  $C_V$  scaled by  $\langle n_i \rangle$  extracted from ALICE data as well as PYTHIA8 as a function of  $\langle dN_{ch}/d\eta \rangle$  for  $\pi^\pm$ ,  $K^\pm$ ,

TABLE I: Average charged-particle pseudorapidity densities corresponding to different event multiplicity classes [44].

Class name	Mul1	Mul2	Mul3	Mul4	Mul5	Mul6	Mul7	Mul8	Mul9	Mul10
$\langle \frac{dN_{ch}}{d\eta} \rangle$	21.3±0.6	16.5±0.5	13.5±0.4	11.5±0.3	10.1±0.3	8.45±0.25	6.72±0.21	5.40±0.17	3.90±0.14	2.26±0.12

$K^{*0} + \bar{K}^{*0}$  and  $p + \bar{p}$  of ALICE data and results from PYTHIA8. It is observed that  $C_V/\langle n_i \rangle$ , (where  $i = \pi^\pm, K^\pm$ ) tend to almost saturate for high-multiplicity, however, a slow variation is observed for  $i = \bar{K}^{*0}$  and  $p + \bar{p}$ . It is important to note that the pionic and kaonic matter (for  $\langle dN_{ch}/d\eta \rangle > 8$ ) have approximately similar value of  $C_V/\langle n_i \rangle$  for both experimental and MC data.

The observed saturation in specific heat in its variation with multiplicity can be attributed to the possibility of thermalization in the system. We also notice that results from PYTHIA8 are not in good agreement with ALICE data for heavier particles like  $K^{*0} + \bar{K}^{*0}$  and  $p + \bar{p}$ . Here  $\langle n_i \rangle$  has a fractional value in unit  $\text{GeV}^3$ , this makes the value of  $C_V/\langle n_i \rangle$  greater than  $C_V$ , as evident from the results displayed in Figs. 6 and Fig 7.

Fig. 8 shows the variation of  $C_V$  (scaled by  $T^3$ ) with  $\langle dN_{ch}/d\eta \rangle$  for  $\pi^\pm, K^\pm, K^{*0} + \bar{K}^{*0}$  and  $p + \bar{p}$  extracted from ALICE data and PYTHIA8. It is observed that  $C_V/T^3$  for  $\pi^\pm, K^\pm, K^{*0} + \bar{K}^{*0}$  increases with multiplicity and display a saturation (within the error bars) when  $\langle dN_{ch}/d\eta \rangle > 8$ , whereas  $p + \bar{p}$  displays an increasing trend with  $\langle dN_{ch}/d\eta \rangle$  without any sign of saturation. This may be a hint to the fact that lower mass particles like  $\pi^\pm, K^\pm$  behave as weakly interacting thermalized particles beyond certain multiplicity, whereas heavier mass particles may not witness a thermalized medium. Here, also PYTHIA8 results are not in good agreement with ALICE data.

Fluid dynamical equation in non-relativistic limit (Euler equation in the limit of small flow velocity ( $v$ ) for ideal fluid) can be written as:  $(\epsilon + P)\partial\vec{v}/\partial t = -\vec{\nabla}P$ , where  $(\epsilon + P)$  is the enthalpy density. Comparison of this equation with the non-relativistic classical mechanical equation of a particle moving with velocity  $v$  in a potential,  $\phi$ :  $m d\vec{v}/dt = -\vec{\nabla}\phi$ , indicates that enthalpy density plays the role of mass (inertia) in fluid dynamics.

Since enthalpy density,  $(\epsilon + P)$ , acts as inertia for change in velocity for a fluid cell in thermal equilibrium, we display the change in  $C_V$  scaled by enthalpy density as a function of multiplicity in Fig 9. The saturations of  $C_V/(\epsilon + P)$  and  $C_V/\langle n_i \rangle$  in their variations with multiplicity show an interesting trend in which, at the saturation region, corresponding values for all the particle species tend to converge. This means that with the increase in the number of particles the system achieved randomization. This is expected when particles in the system evolves collectively with common interaction environment.

The effects of non-extensive parameter,  $q$  on heat capacity has been shown in Fig 10 through the ratio,  $c_v/c_{v,q \rightarrow 1}$ , where,  $c_v = C_V / \langle m_i n_i \rangle$ , here,  $\langle m_i n_i \rangle$  is the mass density of the hadron  $i$ . It may be mentioned

that the  $C_V$  is obtained here by fitting the TB distribution to the ALICE data, therefore,  $C_V$  depends on  $q$ . From Fig 10, the ratio seems to approach toward saturation for  $\langle dN_{ch}/d\eta \rangle > 5$ , implying that new environment of interaction is set-off after  $\langle dN_{ch}/d\eta \rangle \approx (4 - 6)$ , however, the ratio does not approach unity except for  $K^\pm$ . This indicates that the system has not achieved the state to be described by BG statistics.

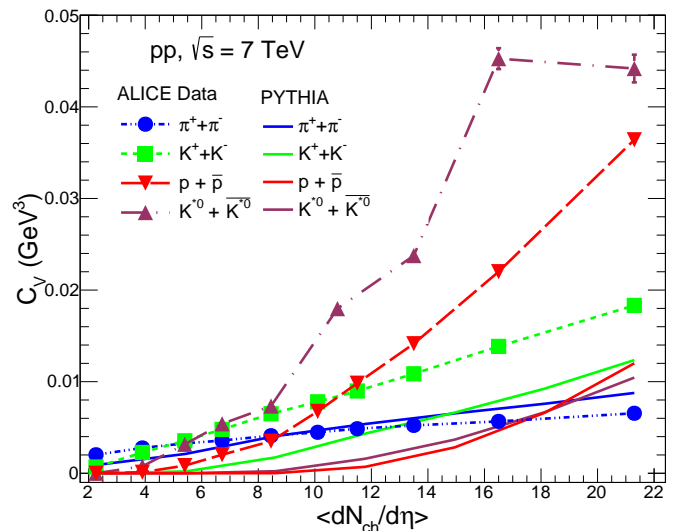


FIG. 6: (Color online) Heat capacity obtained using TB distribution as a function of multiplicity. Dashed (solid) lines represent results obtained using ALICE (PYTHIA8 simulated) data, respectively for  $p + p$  collisions at  $\sqrt{s} = 7$  TeV.

## B. Multiplicity dependence of CSBM, speed of sound and mean transverse momentum

The speed of sound is a useful quantity which helps in characterizing the nature of interaction in a system e.g., whether it is strongly interacting or not, or how much it differs from ideal gas of massless particles. Interaction can cause change in the effective mass of constituents, thereby, changing the speed of sound in the medium. CSBM gives the measure of deviation from masslessness of the constituents (particle mass and temperature dependence of CSBM for weakly interacting system is discussed in [45]). For massless particles,  $c_s^2 = 1/3$ , however for massive particles,  $c_s^2 < 1/3$ . This is due to the fact that the massive particles do not contribute to the change in pressure as much as they contribute to the change in energy of the system. Variation of these quantities with

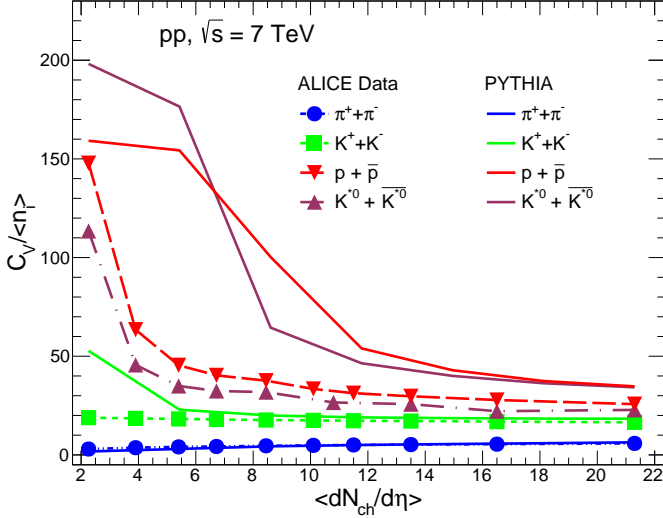


FIG. 7: (Color online) Same as Fig. 6 showing the variation of  $C_V / \langle n_i \rangle$  with charged multiplicity.

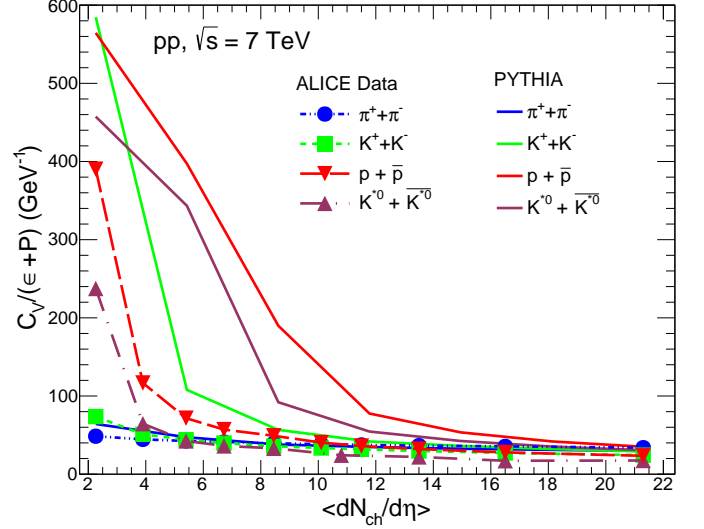


FIG. 9: (Color online) Same as Fig. 6 showing the variation of  $C_V / (\epsilon + P)$  with charged multiplicity.

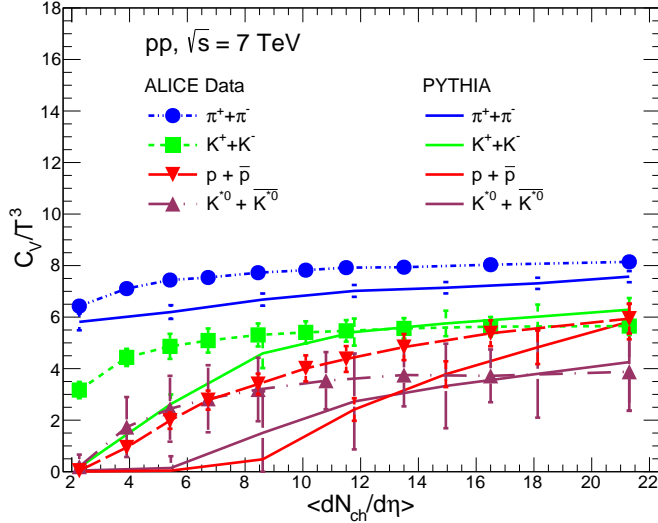


FIG. 8: (Color online) Same as Fig. 6 showing the variation of  $C_V / T^3$  with charged multiplicity.

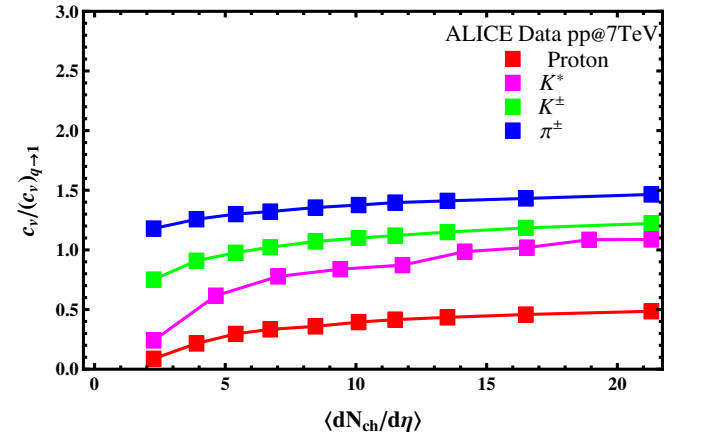


FIG. 10: (Color online) Heat capacity scaled by the mass density is plotted as a function of charged particle multiplicity (see text). The errors are within the marker size.

multiplicity is expected to capture the change in effective interaction among constituents with increase in number of constituents. Also the variation of  $\langle p_T \rangle$  of a system with the number of constituents can capture the onset of thermalization in the system.

Variation of CSBM,  $c_s^2$  and  $\langle p_T \rangle$  with multiplicity for  $p + p$  collisions have been estimated with the help of Eqs. 10, 11, 13 respectively.

It may be noted here that  $(\epsilon - 3P)$  is zero for massless ideal gas, therefore, its non-zero value is a measure of interaction in the system. Fig. 11 shows variation of CSBM  $[\sim (\epsilon - 3P)/T^4]$  of  $\pi^\pm$ ,  $K^\pm$ ,  $K^{*0} + \bar{K}^{*0}$  and  $p + \bar{p}$  with  $\langle dN_{ch}/d\eta \rangle$ . It is observed that the CSBM for pi-

ons slowly reduces and as multiplicity increases while for kaons and  $K^*$  it shows almost remains constant for  $\langle dN_{ch}/d\eta \rangle > 5$  (within error bars). CSBM displays an increasing behaviour with  $\langle dN_{ch}/d\eta \rangle > 5$ . In comparison with PYTHIA8 generated results, we observed that  $\pi^\pm$  and  $K^\pm$  trend underestimates the ALICE data while to some extent PYTHIA8 explains  $K^{*0} + \bar{K}^{*0}$  and  $p + \bar{p}$ . It is expected that for a thermalized medium, the contribution of a hadron of particular species to CSBM peaks when the temperature of the system is half of its mass [45]. The value of  $T$  obtained from the present analysis is less than 190 MeV [43]. Therefore, for pions the peak in CSBM can be achieved for  $T \geq m_\pi/2$ . However, all other hadrons can not achieve the peak in CSBM as they are heavy and  $T < m_H/2$ , where  $m_H$  is mass of the hadrons heavier

than pion. The larger values of CSBM indicates significant amount of interactions among hadrons or pressure is low in the non-relativistic limit.

Fig. 12 shows the variation of  $c_s^2$  (Eq. 11) of  $\pi^\pm$ ,  $K^\pm$ ,  $K^{*0} + \bar{K}^{*0}$  and  $p + \bar{p}$  as a function of  $\langle dN_{ch}/d\eta \rangle$ . It is observed that as we move from low to high-multiplicity of ALICE data, the  $c_s^2$  for  $\pi^\pm$  almost remains constant, while  $c_s^2$  for  $K^\pm$  increases upto  $\langle dN_{ch}/d\eta \rangle \approx 4$  and then saturates.  $c_s^2$  for  $K^{*0} + \bar{K}^{*0}$  and  $p + \bar{p}$  increase with multiplicity. It is also observed that PYTHIA8 overestimates the ALICE data. As expected, low mass particles will have higher  $c_s^2$  than heavier mass particles. The saturated value of  $c_s^2$  beyond  $\langle dN_{ch}/d\eta \rangle \approx 6$  follows the mass ordering. The results obtained from PYTHIA8 data, however, is less than the values obtained from experimental data.

Fig. 13 shows  $\langle p_T \rangle$  of  $\pi^\pm$ ,  $K^\pm$ ,  $K^{*0} + \bar{K}^{*0}$  and  $p + \bar{p}$  as a function of  $\langle dN_{ch}/d\eta \rangle$  for ALICE data and PYTHIA8 generated results estimated using Eq. 13 with lower limit of integration varying from 0.17 to 0.22 GeV/c to reproduce the  $\langle p_T \rangle$  reported in Ref. [44] (this limit on integration is now used for all other calculations for  $\langle p_T \rangle$ , which have no apparent effect on other observables considered here). It is observed that  $\langle p_T \rangle$  of all hadrons increase very slowly as multiplicity increases. The higher are the mass of hadrons, the higher are the values of  $\langle p_T \rangle$ . This may be indicative of the presence of collectivity in the system through transverse flow as higher mass hadrons get affected by the flow more ( $p_T \sim mv_T$  where  $m$  is the mass of the hadrons and  $v_T$  is the transverse flow velocity).

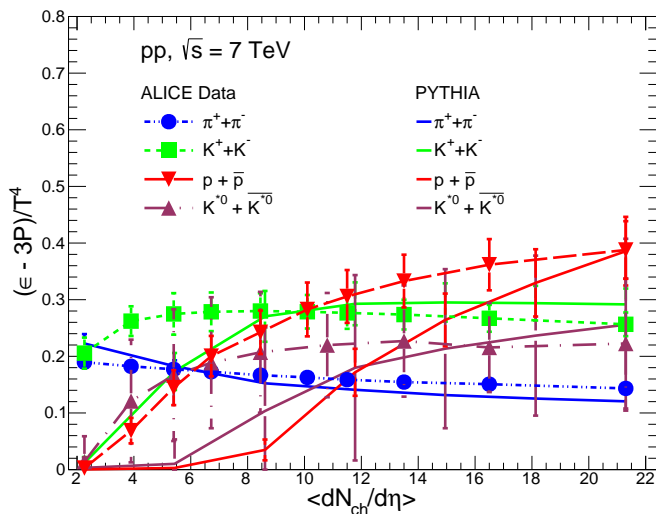


FIG. 11: (Color online) Variation of CSBM with  $\langle dN_{ch}/d\eta \rangle$  is shown. Dashed (solid) lines represent results obtained by using ALICE data (PYTHIA8 simulation) for  $p + p$  collisions at  $\sqrt{s} = 7$  TeV.

It is interesting to find that all of the above quantities for lighter hadrons show saturation for  $\langle dN_{ch}/d\eta \rangle \geq (4-6)$  in their variation with  $\langle dN_{ch}/d\eta \rangle$ . This general

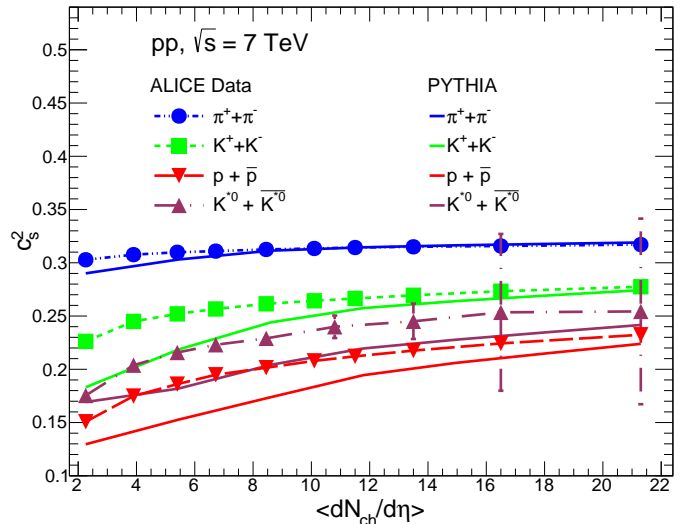


FIG. 12: (Color online) Same as Fig. 11 for speed of sound.

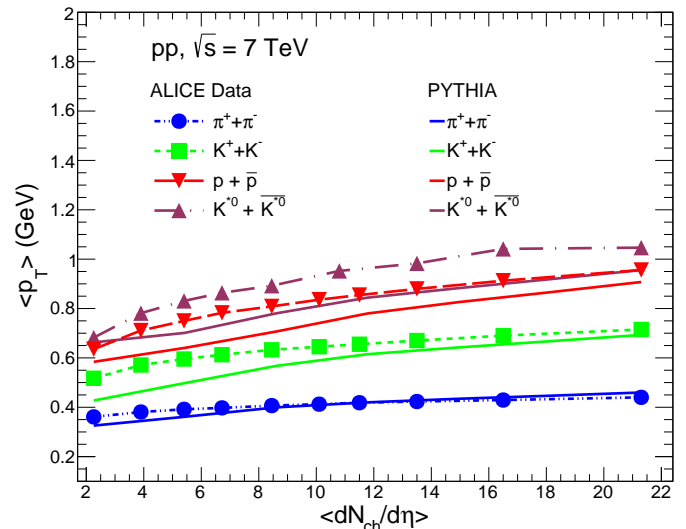


FIG. 13: (Color online) Mean transverse momentum in GeV is presented as a function of charged particle multiplicity. Dashed (solid) lines are obtained by using ALICE data (PYTHIA8 simulation).

feature may be the hint of onset of their possible randomized collective nature. This is more prominent in the variation of speed of sound and CSBM with multiplicity, where heavier hadrons show different trends from that of lighter hadrons. Moreover, the saturation found here is vastly different from the saturation of  $\langle p_T \rangle$  of all charged particles which occurs at  $\langle dN_{ch}/d\eta \rangle \approx 20$  as in Ref. [21]. This may be due to the inclusion of heavier particles in calculation of  $\langle p_T \rangle$ . In fact, in this work, it is found that heavier particles like proton shows different nature; for them instead of saturation, quantities considered here in-



creases monotonically. It is also interesting to note that heavier hadrons are described well by PYTHIA8. It further emboldens the possibility of formation of strongly correlated but randomized medium, as this can not be explained by color reconnection (CR) effect of final state which is included in PYTHIA8. This mismatch points out something more than CR effect is responsible for such saturation, hinting scope of presence of collectivity in the system from which these particles originate.

### C. Finite system size dependence of heat capacity

In case of RHICE, the thermal nature of produced particles is extensive type (BG), but for  $p + p$  collisions, Tsallis (TB) distribution fits the particle spectra very well [46, 47]. The appearance of non-extensive statistics in a system may be for several reasons e.g., finite size effect, long-range interaction or correlation. For this reason, in this work, it is investigated whether finite size effect alone can explain the deviation of the value of  $q$  from unity. We incorporate the finite-size effect by considering a lower momentum cutoff,  $p_{min} = \pi/R$ , in the momentum integration, where,  $R$  is the radius of the system [48]. As the collision energy is the same, large multiplicity events are expected to be originating from larger overlap region in  $p + p$  collisions. We have considered different radius ( $R$ ) with each multiplicity following the relation  $R \sim \langle dN_{ch}/d\eta \rangle^{1/3}$  [49–51]. The  $R$  dependence of  $C_V$ , CSBM,  $c_s$  and  $\langle p_T \rangle$  have been extracted by fitting data from  $p + p$  collision at  $\sqrt{s} = 7$  TeV to TB distribution with  $T$  and  $q$  as fitting parameters. The data sets have also been studied by using BG statistics (in the limit  $q \rightarrow 1$ ) with the same value of  $T$  obtained from TB statistics, to check whether extensive TB distribution with finite size effect can account for the  $q$ -value extracted by fitting experimental data.

In order to account for the effects of system size, we have studied variation of heat capacity, heat capacity scaled by average number of particles and  $T^3$  with finite system size using Eq. 9. We find the lower limit of  $R$  as 1.3 fm and the upper limit to be 2.7 fm. This is used to represent the available multiplicity classes such that the values with  $q \neq 1$  same as that of earlier plots showing variation with multiplicity. Finite system size is also reflected through the value of  $q > 1$  in contrast to  $q \rightarrow 1$ .

Fig. 14 shows  $C_V$  of  $\pi^\pm$ ,  $K^\pm$ ,  $K^{*0} + \overline{K^{*0}}$  and  $p + \bar{p}$  obtained by using ALICE data as a function of system size. It is observed that the  $C_V$  of  $\pi^\pm$ ,  $K^\pm$  and  $p + \bar{p}$  increases with system size for  $q \neq 1$ . The slope of  $C_V$  for  $\pi^\pm$  is less compared to  $K^\pm$  and  $p + \bar{p}$ . Results with  $q \rightarrow 1$  (corresponding to BG statistics) represented by solid curves indicate that  $C_V$  of  $K^\pm$ ,  $p + \bar{p}$  are underestimated by PYTHIA8 unlike  $\pi^\pm$ .

Fig. 15 shows  $C_V$  scaled by  $T^3$  for  $\pi^\pm$ ,  $K^\pm$ ,  $K^{*0} + \overline{K^{*0}}$  and  $p + \bar{p}$  extracted from ALICE data as a function of system size. It is observed that  $C_V/T^3$  for  $\pi^\pm$ ,  $K^\pm$ ,

$K^{*0} + \overline{K^{*0}}$  and  $p + \bar{p}$  vary slowly with increasing system size for both with TB and BG statistics (except for  $p + \bar{p}$ ).

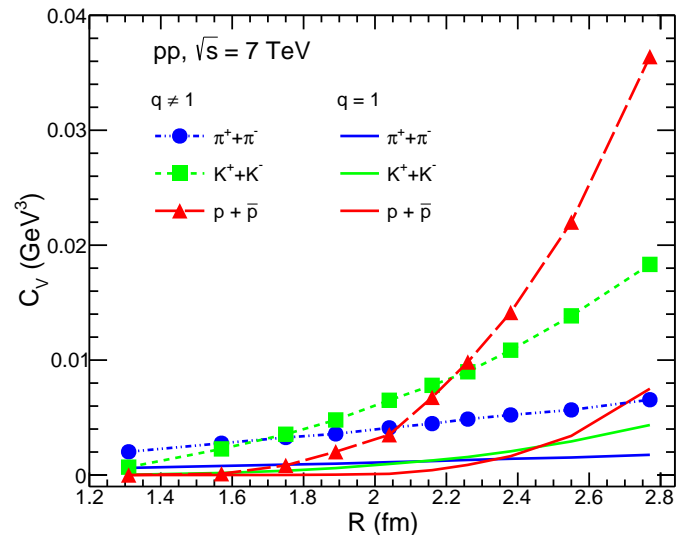


FIG. 14: (Color online) Heat capacity obtained by using BG and TB distribution as a function of system size. Dashed (solid) lines represent results for  $q \neq 1$  ( $q = 1$ ) for  $p + p$  collisions at  $\sqrt{s} = 7$  TeV.

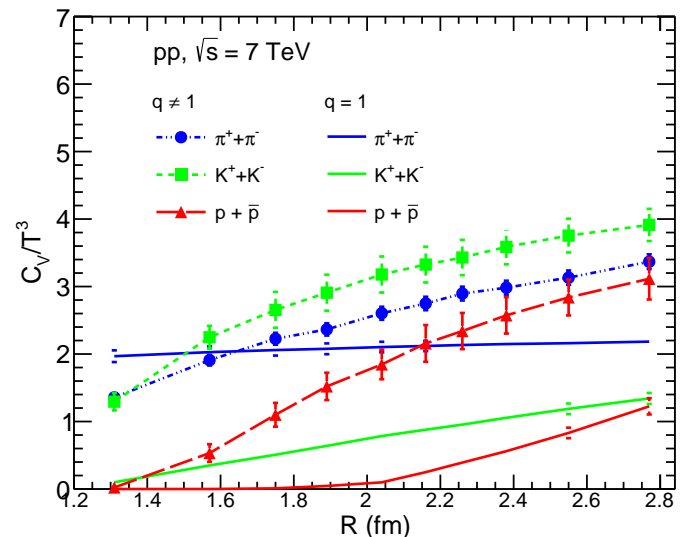


FIG. 15: (Color online) Same as Fig. 14 for heat capacity scaled by  $T^3$ .

### D. Finite system size dependence of CSBM, speed of sound and mean transverse momentum

Fig. 16 shows CSBM of  $\pi^\pm$ ,  $K^\pm$  and  $p + \bar{p}$  obtained from ALICE data as a function of system size. Results

with  $q \neq 1$  represented by dashed lines, it is observed that CSBM of  $\pi^\pm$  decreases slowly while CSBM of  $K^\pm$  increases slightly at small  $R$ . But  $p + \bar{p}$  displays an increasing trend. Results for BG statistics represented by solid curves show similar trend. It may be noted that the heavier hadrons contribute more to the energy density than pressure through their rest mass energy, therefore for proton ( $\epsilon - 3P$ ) will be more than pions.

Fig. 17 shows  $c_s^2$  for  $\pi^\pm$ ,  $K^\pm$ ,  $K^{*0} + \bar{K}^{*0}$  and  $p + \bar{p}$  extracted from ALICE data as a function of system size. The  $c_s^2$  shows a plateau as a function of  $R$  both for BG and TB statistics for all the hadronic species.

Fig. 18 shows  $\langle p_T \rangle$  for  $\pi^\pm$ ,  $K^\pm$ ,  $K^{*0} + \bar{K}^{*0}$  and  $p + \bar{p}$  of ALICE data as a function of system size. For TB statistics, it is observed that  $\langle p_T \rangle$  of all hadrons increases with system size (faster for  $p + \bar{p}$ ) and reaches a plateau beyond  $R \sim 1.8$  fm. In BG statistics,  $\pi^\pm$  and  $K^\pm$  show slow variation.

It is generally observed that the incorporation of finite size effect in BG statistical approach can not reproduce the value of the observables calculated with non-extensivity parameter ( $q$ ) extracted from the  $p + p$  collisions. This may suggest that the appearance of non-extensivity in  $p + p$  collisions may not be completely explained by finite size effect alone, thereby hinting the presence of other physical effects like long-range correlation that also contributes to the origin of non-extensivity.

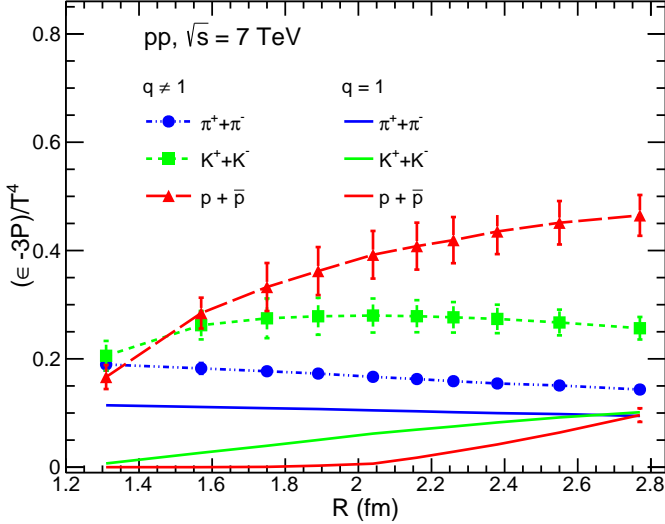


FIG. 16: (Color online) Same as Fig. 14 showing variation of CSBM with  $R$ .

### E. Energy dependence of $C_V$ , CSBM, $c_s^2$

The collision energy dependence of heat capacity scaled by average number of particles and  $T^3$  obtained from RHICE and ALICE  $p + p$  data at different  $\sqrt{s}$  has been studied by using the values of  $T$  and  $q$  extracted from

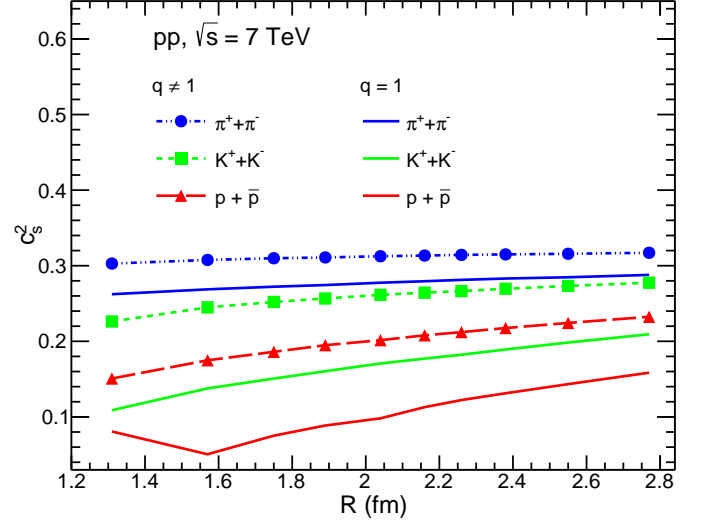


FIG. 17: (Color online) Same as Fig. 14 for  $c_s^2$ .

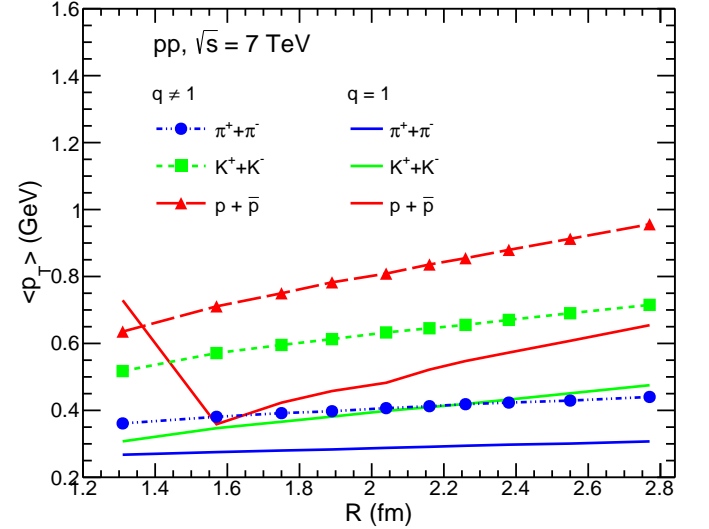


FIG. 18: (Color online) Same as Fig. 14 for  $\langle p_T \rangle$ .

the TB distribution fit of the  $p_T$ -spectra [52], where  $\sqrt{s}$  ranges from 0.0624 TeV to 13 TeV.

Fig. 19 shows  $C_V$  scaled by the average density of charged pions ( $\langle n_\pi \rangle = \langle n_{\pi^+} \rangle + \langle n_{\pi^-} \rangle$ ) as a function of  $\sqrt{s}$ . Here, scaling by  $\langle n_\pi \rangle$  is considered as production of ( $\pi^+$  and  $\pi^-$ ) is abundant in relativistic collisions. It is observed that  $C_V/\langle n_\pi \rangle$  increases sharply upto  $\sqrt{s} = 1.5$  TeV beyond which it increases very slowly. In the same figure we also display the variations of  $C_V/T^3$  and CSBM of charged particles obtained from RHICE and ALICE data as a function of  $\sqrt{s}$ . Both the quantities tend to saturate (within error bars) for  $\sqrt{s} > 2$  TeV. We find that speed of sound seems to be almost constant (Fig. 19) for  $\sqrt{s} > 2$  GeV. Possibly for  $p+p$  collisions with  $\sqrt{s} \leq 2$  TeV

a thermal medium is formed with the value of  $c_s^2 \approx 0.24$ . Such a value of  $c_s^2$  is obtained in hadronic resonance gas model calculation [45].

The general observation in this regard is that the thermodynamic quantities considered here show a saturation starting for  $\sqrt{s} \geq 2$  TeV. The nature of variation of  $C_V/\langle n_\pi \rangle$  beyond  $\sqrt{s} \approx 2$  TeV is similar to that found in heavy-ion collisions at the chemical-freeze out surface as in Ref. [23]. Therefore, this may be taken as a hint for the formation of medium similar in kind to that of heavy-ion collisions. Indicating that for  $\sqrt{s} \geq 2$  TeV sufficient number of particles are produced to form QCD medium. It is interesting to further note that the average multiplicity for  $\sqrt{s} \approx 1.5$  lies between 3 to 7 as in Ref. [53]. This again puts weight to the possibility that the saturation effect as observed in variation of above thermodynamic quantities with multiplicity is potentially due to formation of a medium in  $p+p$  collisions for multiplicity,  $\langle dN_{\text{ch}}/d\eta \rangle \geq 4-6$ . We note that for observing saturation effects in PYTHIA8 simulated results (in which CR is thought to be responsible for the saturation), this kind of saturation starts at  $\langle dN_{\text{ch}}/d\eta \rangle \approx 20$ .

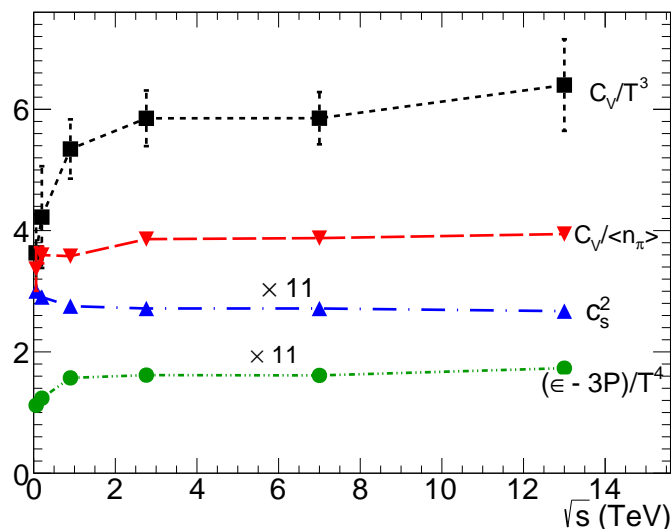


FIG. 19: (Color online) Variation of heat capacity scaled by  $T^3$  and average charged pion density ( $\langle n_\pi \rangle$ ), speed of sound and CSBM with  $\sqrt{s}$  for  $p+p$  collisions.

## V. SUMMARY

The findings of the present work based on the analysis of data from  $p+p$  collision at LHC energies may be summarized as follows:

- We have analyzed how a system produced in  $p+p$  collision at relativistic energies evolves into a collective medium as the the number of produced particles and collision energy increases. For the purpose

of this analysis, the thermodynamic quantities like  $C_V$ ,  $c_s$  and CSBM have been chosen for reasons explained in the text. We observe that  $C_V$  achieves a plateau for  $\langle dN_{\text{ch}}/d\eta \rangle > (4-6)$ . We also note that  $C_V/\langle n_i \rangle$  for pionic and kaonic matter have similar values.

- We have also investigated how conformal symmetry breaking/trace anomaly varies with the degrees of freedom in an environment of QCD many body system. Similar to  $C_V$ , a saturation in CSBM with  $\langle dN_{\text{ch}}/d\eta \rangle$  and  $\sqrt{s} \geq 2$  TeV is also observed.
- The importance of high-multiplicity ( $\langle dN_{\text{ch}}/d\eta \rangle > (4-6)$ ) for medium formation in small systems is further endorsed by the observation of similar kind of saturating behaviour of the thermodynamic quantities considered here with collision energies. This suggests that at collision energies,  $\sqrt{s} \geq 2$  TeV, the sea quarks and gluons within the proton are large enough to produce QCD medium.
- Comparisons of the results extracted from ALICE data with the results obtained from PYTHIA8 simulation have been carried out. It is observed that PYTHIA8 (devoid of medium) explains scaled  $C_V$  for heavy particles approximately but it cannot explain the trend of lighter hadrons. This may be a sign that lower mass particles originate from a thermalized medium.
- The deviation in the value of  $q$  from unity in TB statistics may indicate the presence of long-range correlations as well as the finiteness of the system. However, it is observed that finite size effect alone cannot account for the appearance of  $q \neq 1$  value. This may suggest that the presence of effects other than finiteness *e.g.*, correlations, in QCD system play important role for giving rise to non-extensivity.

## VI. ACKNOWLEDGEMENT

SD, GS and RNS acknowledge the financial supports from ALICE Project No. SR/MF/PS-01/2014-IITI(G) of Department of Science & Technology, Government of India. Further, R.S. acknowledges the financial supports from DAE-BRNS Project No. 58/14/29/2019-BRNS. JA is grateful to Tramabak Bhattacharyya for useful discussions.

- 
- [1] R. Baier, P. Romatschke and U. A. Wiedemann, Phys. Rev. C **73**, 064903 (2006).
- [2] B. Alver *et al.* [PHOBOS Collaboration], Phys. Rev. C **81**, 034915 (2010).
- [3] B. Z. Kopeliovich, I. K. Potashnikova and I. Schmidt, Nucl. Phys. A **864**, 203 (2011).
- [4] G. Agakishiev *et al.* [STAR Collaboration], Phys. Rev. Lett. **108**, 072301 (2012).
- [5] T. Isobe [PHENIX Collaboration], nucl-ex/0605016.
- [6] V. Khachatryan, *et al.*, CMS, J. High Energy Phys. **09**, 091 (2010).
- [7] W. Li, Mod. Phys. Lett. A **27**, 1230018 (2012).
- [8] V. Khachatryan, *et al.*, CMS, Phys. Rev. Lett. **116**, 172302 (2016).
- [9] G. Aad, *et al.*, ATLAS, Phys. Rev. Lett. **116**, 172301 (2016).
- [10] V. Khachatryan, *et al.*, CMS, Phys. Lett. B **765**, 193 (2017).
- [11] W. Zhao, Y. Zhou, H. Xu, W. Deng and H. Song, Phys. Lett. B **780**, 495 (2018).
- [12] M. Mace, V.V. Skokov, P. Tribedy, R. Venugopalan, Phys. Rev. Lett. **121**, 052301 (2018).
- [13] M. A. Braun, J. Dias de Deus, A. S. Hirsch, C. Pajares, R. P. Scharenberg and B. K. Srivastava, Phys. Rept. **599**, 1 (2015).
- [14] L. D. Landau, Izv. Akad. Nauk. SSSR **17**, 51 (1953); S. Belenkij and L. D. Landau, Usp. Fiz. Nauk. **56**, 309 (1955); Nuovo Cimento Suppl. **3**, 15 (1956); D. ter Haar (Ed.), Collected papers of L.D. Landau, Gordon & Breach, New York, 1965, p. 665.
- [15] L. Van Hove, Phys. Lett. **118B**, 138 (1982).
- [16] R. P. Scharenberg, B. K. Srivastava and C. Pajares, Phys. Rev. D **100**, 114040 (2019).
- [17] S. Borsanyi *et al.*, JHEP **1011**, 077 (2010).
- [18] S. Borsanyi *et al.*, J. Phys: Conf. Series **316**, 012020 (2011).
- [19] D. Thakur [ALICE Collaboration], PoS HardProbes 2018, **164** (2019).
- [20] D. Adamová *et al.* [ALICE Collaboration], Phys. Lett. B **776**, 91 (2018).
- [21] B. Abelev *et al.* for ALICE Collaboration, Physics Letters B **727** 371 (2013).
- [22] J. Adams *et al.* Nature Physics **13**, 535 (2017).
- [23] S. Basu, S. Chatterjee, R. Chatterjee, T. K. Nayak and B. K. Nandi, Phys. Rev. C **94**, 044901 (2016).
- [24] X. M. Li, S. Y. Hu, J. Feng, S. P. Li, B. H. Sa and D. M. Zhou, Int. J. Mod. Phys. E **16**, 1906 (2007).
- [25] Reif, F., Fundamentals of Statistical and Thermal Physics, McGraw-Hill International Editions, Singapore, 1985.
- [26] E. W. Kolb and M. S. Turner, The Early Universe, Addison-Wesley Publishing Co., Singapore, 1989.
- [27] J. Cleymans, AIP Conf. Proc. **1625**, 31 (2015).
- [28] C. Tsallis, J. Statist. Phys. **52**, 479 (1988).
- [29] C. Tsallis, Eur. Phys. J. A **40**, 257 (2009).
- [30] C. Tsallis, Introduction to Nonextensive Statistical Mechanics (Springer, 2009).
- [31] G. Wilk, and Z. Włodarczyk, Phys. Rev. Lett. **84**, 2770 (2000).
- [32] G. Wilk, and Z. Włodarczyk, Phys. Rev. C **79**, 054903 (2009).
- [33] G. Wilk, and Z. Włodarczyk, Chaos Solitons Fractals **13**, 581 (2001).
- [34] J. Cleymans and D. Worku, Eur. Phys. J. A **48**, 160 (2012).
- [35] S. K. Tiwari, S. Tripathy, R. Sahoo and N. Kakati, Eur. Phys. J. C **78**, 938 (2018).
- [36] T. Sjostrand, S. Mrenna and P. Z. Skands, JHEP **0605**, 026 (2006).
- [37] PYTHIA8 online manual:(<http://home.thep.lu.se/~torbjorn/PYTHIA8>)
- [38] A. Ortiz Velasquez, P. Christiansen, E. Cuautle Flores, I. Maldonado Cervantes and G. Paić, Phys. Rev. Lett. **111**, 042001 (2013).
- [39] R. Corke and T. Sjostrand, JHEP **1103**, 032 (2011).
- [40] G. Aad *et al.* [ATLAS Collaboration], New J. Phys. **13**, 053033 (2011).
- [41] B. C. Li, Z. Zhang, J. H. Kang, G. X. Zhang and F. H. Liu, Adv. High Energy Phys. **2015**, 741816 (2015).
- [42] D. Thakur, S. Tripathy, P. Garg, R. Sahoo and J. Cleymans, Adv. High Energy Phys. **2016**, 4149352 (2016).
- [43] A. Khuntia, H. Sharma, S. Kumar Tiwari, R. Sahoo and J. Cleymans, Eur. Phys. J. A **55**, 3 (2019).
- [44] S. Acharya *et al.* [ALICE Collaboration], Phys. Rev. C **99**, 024906 (2019).
- [45] G. Sarwar, S. Chatterjee and J. Alam, J. Phys. G **44**, 055101 (2017).
- [46] L. Marques, J. Cleymans and A. Deppman, Phys. Rev. D **91**, 054025 (2015).
- [47] J. Cleymans, EPJ Web Conf. **70**, 00009 (2014).
- [48] A. Bhattacharyya, R. Ray, S. Samanta and S. Sur, Phys. Rev. C **91**, 041901 (2015).
- [49] K. Aamodt *et al.* [ALICE Collaboration], Phys. Lett. B **696**, 328 (2011).
- [50] B. B. Abelev *et al.* [ALICE Collaboration], Phys. Lett. B **739**, 139 (2014).
- [51] J. Adam *et al.* [ALICE Collaboration], Eur. Phys. J. C **76**, 245 (2016).
- [52] K. Saraswat, P. Shukla and V. Singh, J. Phys. Comm. **2**, 035003 (2018).
- [53] A. Alkin, Ukr. J. Phys. **62**, 743 (2017).